

Large-Scale, Solution-Phase Growth of Single-Crystalline SnO₂ Nanorods

Bin Cheng,[†] Joette M. Russell,[†] Wensheng Shi,[†] Lei Zhang,[‡] and Edward T. Samulski^{*†‡}

Department of Chemistry and Curriculum in Applied & Materials Sciences, University of North Carolina, Chapel Hill, North Carolina 27599-3290

Received February 6, 2004; E-mail: et@unc.edu

In this Communication, we report for the first time a solution route to single-crystalline SnO₂ nanorods with dimensions approaching those of molecules (diameter ~3.4 nm) and comparable in size to the smallest diameter nanowires reported to date.¹ Driven by putative applications in nanoelectronics, facile routes to one-dimensional (1-D) nanostructures (nanorods, nanowires and nanotubes) are actively being pursued.^{2–5} Methods ranging from virus-templating⁶ and biomolecular-assisted synthesis⁷ to conventional solution-phase precursor routes⁸ have been employed to fabricate 1-D nanostructures. Especially important are metal oxide nanostructures which can exhibit tunable electrical, optical, magnetic, and chemical properties.⁹ The wide band gap ($E_g = 3.6$ eV) semiconductor SnO₂ is a case in point, with potential technological applicability in gas sensors,¹⁰ transparent conducting electrodes,¹¹ transistors, and solar cells.¹² The general synthetic approaches for 1-D SnO₂ nanostructures include thermal evaporation,^{4,13} laser ablation,¹⁴ solution-phase growth,¹⁵ and template-based methods.¹⁶

Although solution-phase growth has distinct advantages, using this route to isolated single nanocrystals of SnO₂ has not been successful. Zhang et al.¹⁵ have shown that relatively large dendritic crystals (10 × 200 nm) can be prepared via a 200 °C solution route, and Wang et al.⁸ have recently reported polycrystalline SnO₂ nanowires (~50 nm diameter) derived from a solution synthesis (refluxing at ~200 °C) followed by an annealing step at 500 °C. Herein, we report small-diameter, single-crystalline SnO₂ nanorods synthesized in alcohol–water mixtures at 150 °C.

In a typical procedure, an Sn⁴⁺ precursor (SnCl₄·5H₂O, 0.001 mol) was dissolved in a basic mixture of alcohol and water (pH ≈ 12). The clear solution with dissolved precursor was transferred to a Teflon-lined stainless steel autoclave and heated at 150 °C for 24 h. A white-gray precipitate was collected, purified, and dried in air at ambient temperature with a yield ≈100%. The synthesized SnO₂ nanorods were characterized by X-ray powder diffraction (XRD) (Rigaku Multiflex X-ray diffractometer, with Cu K α radiation ($\lambda = 0.154178$ nm at 40 kV and 40 mA)), transmission electron microscopy (TEM; JEOL JEM-100CXII, with an accelerating voltage of 100 kV), and high-resolution transmission electron microscopy (HRTEM; JEOL JEM-2010F, with an accelerating voltage of 200 kV).

The morphology, structure, and size of the SnO₂ nanorods were characterized with TEM and HRTEM. The size distribution analysis is presented in the supplementary information (Figure S1). Figure 1(A) is a wide-field TEM image of the as-prepared SnO₂ nanorods that clearly indicates that the product is entirely comprised of a relatively uniform, rodlike morphology (15–20 nm rod lengths and 2.5–5 nm rod diameters). The inset on the lower right shows a magnified view of laterally aggregated nanorods. The upper right inset shows a selected area electron diffraction (SAED) pattern from an individual nanorod with a [1-10] zone axis, which indicates

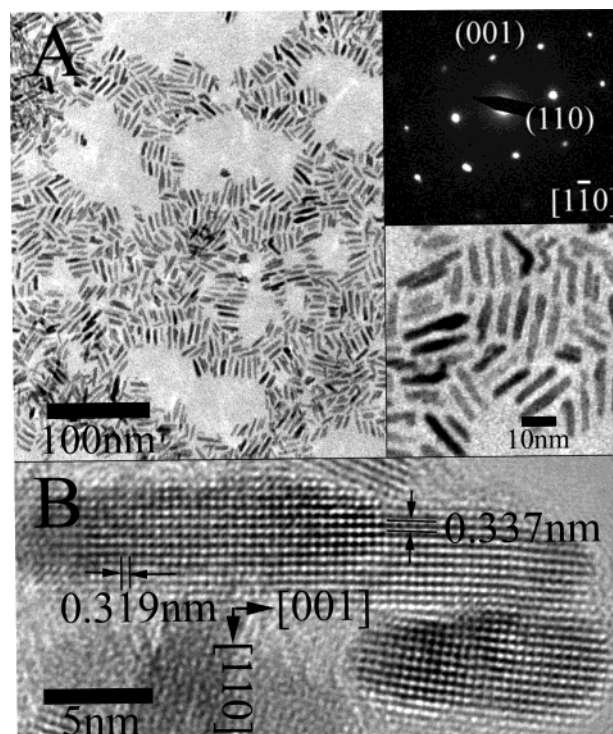


Figure 1. (A) TEM image of the as-prepared SnO₂ nanorods. The lower right inset shows laterally aggregated nanorods; the upper right inset is a SAED pattern from an individual nanorod. (B) HRTEM image of the SnO₂ nanorods, showing a clear two-dimensional lattice with the [001] direction along the nanorod major axis.

that the as-prepared SnO₂ nanorods are single-crystalline. The lattice fringes in the HRTEM image (Figure 1B) further confirm the single-crystal nature of the SnO₂ nanorods. The spacing between adjacent lattice planes is 0.337 nm, corresponding to (110) planes of rutile SnO₂, which indicates that the preferential growth direction is [001]. The mean rod length (17 ± 4 nm) and diameter (3.4 ± 0.6 nm) extracted from TEM image of more than 300 nanorods (Figure S1).

Figure 2 shows the powder X-ray diffraction (XRD) pattern from the as-prepared product. The diffraction peaks are quite similar to those of bulk SnO₂, which can be indexed as the tetragonal rutile structure of SnO₂ with lattice constants of $a = 4.74$ Å and $c = 3.18$ Å. (This is in good agreement with the JCPDS file of SnO₂ (JCPDS 41-1445).) No impurity peaks were observed, indicating the high purity of the final products. However, the peaks were relatively broad compared with those of the bulk material, corroborating the very small crystal size.

An analysis of the surface energies in different crystallographic orientations gives information about relative growth rates of the different crystal facets. Several groups have used different methods^{18–20} to calculate the specific surface energies of crystalline SnO₂. Their calculations exhibit the same general trends, i.e., in

[†] Department of Chemistry.

[‡] Curriculum in Applied & Materials Science.

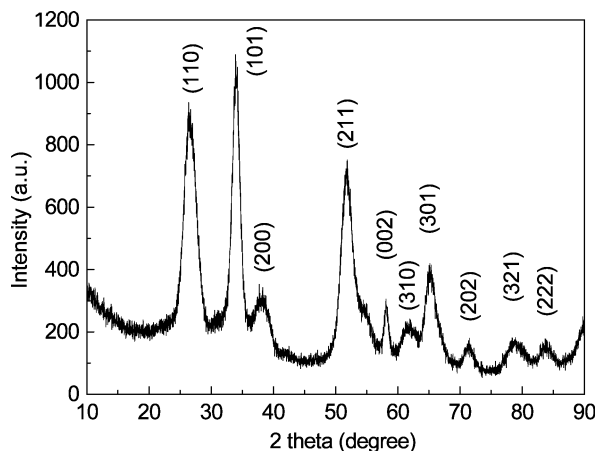


Figure 2. X-ray diffraction (XRD) pattern of the SnO₂ nanorods.

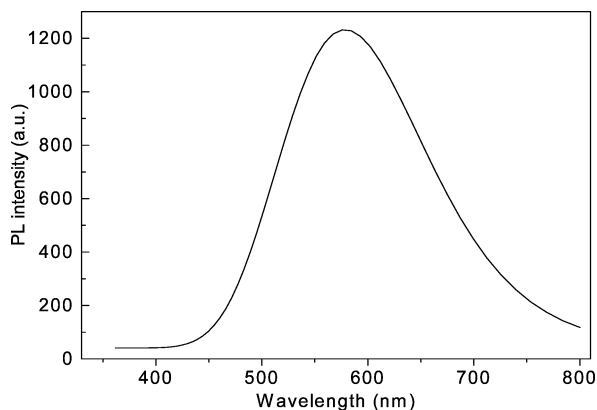


Figure 3. Room-temperature photoluminescence spectrum of the as-prepared SnO₂ nanorods.

order of increasing energy, the surfaces form the sequence (110) < (100) < (101) < (001). Since the (110) and (001) surfaces are suggested to have the lowest and the highest surface energies, respectively, and the [001] direction is the favored growth direction and should result in particles with a high aspect ratio. Our experimental findings for SnO₂ nanorods agree very well with these calculations, i.e., the single-crystalline nanorods show a mean aspect ratio of ~ 4:1 with the [001] direction along the major axis.

Raman spectroscopy is also sensitive to crystal surface area. Figure S2 shows that the room-temperature Raman spectrum of the SnO₂ nanorods has bands at 576 and 356 cm⁻¹ in addition to the A_{1g} vibration mode at 631 cm⁻¹. However, the phonon modes of the first two bands are not observed in Raman spectra of bulk single crystal and polycrystalline SnO₂. These modes, being related to the facet surface area of a crystal, arise from nanoscale SnO₂ with small grain size. This finding agrees very well with the Matossi force constant model.²¹ The Raman bands confirm the characteristics of the tetragonal rutile structure as well as the very small size of the SnO₂ nanorods.

Figure 3 shows the room-temperature photoluminescence spectrum of the as-prepared SnO₂ nanorods. A red emission at 580 nm was observed from the SnO₂ nanorods using a He–Cd laser (~325

nm) as the excitation source. The low-energy emission might be related to crystal defects or defect levels associated with oxygen vacancies, or tin interstitials that have formed during growth. A similar red emission has been reported in the case of SnO₂ nanoribbons synthesized by laser ablation.¹⁴

In summary, small diameter, single-crystalline SnO₂ nanorods were prepared in solution at low temperature without using catalysts. The single-crystalline SnO₂ nanorods show a mean aspect ratio of 4:1 with the [001] direction along the major axis. The optical measurements further show that the SnO₂ nanorods possess surface characteristics that generate a red emission band that may be exploited in gas sensors or other optoelectronic devices.

Acknowledgment. This work is supported by the NASA University Research, Engineering and Technology Institute on Bio Inspired Materials (BIMat) under Award No. NCC-1-02037. We thank Dr. Qi Zhang for HRTEM and Jennifer Weinberg-Wolf for Raman measurements.

Supporting Information Available: Length and diameter distribution of the single-crystalline SnO₂ nanorods (Figure S1); Raman spectrum of the SnO₂ nanorods (Figure S2). This material is available free of charge via the Internet at <http://pubs.acs.org>.

References

- (1) Wu, Y.; Cui, Y.; Huynh, L.; Barrelet, C. J.; Bell, D. C.; Lieber, C. M. *Nano Lett.* **2004**, *4*, 433.
- (2) Zhong, Z.; Wang, D.; Cui, Y.; Bockrath, M.; Lieber, C. *Science* **2003**, *302*, 1377.
- (3) (a) Duan, X.; Niu, C.; Sahi, V.; Chen, J.; Parce, J.; Empedocles, S.; Goldman, J. *Nature* **2003**, *425*, 274. (b) Duan, X.; Huang, Y.; Agarwal, R.; Lieber, C. *Nature* **2003**, *421*, 241.
- (4) Pan, Z. W.; Dai, Z. R.; Wang, Z. L. *Science* **2001**, *291*, 1947.
- (5) Huang, M.; Mao, S.; Feick, H.; Yan, H.; Wu, Y.; Kind, H.; Weber, E.; Russo, R.; Yang, P. *Science* **2001**, *292*, 1897.
- (6) Mao, C.; Solis, D. J.; Reiss, B. D.; Kottmann, S. T.; Sweeney, R. Y.; Hayhurst, A.; Georgiou, G.; Iverson, B.; Belcher, A. M. *Science* **2004**, *303*, 213.
- (7) Lu, Q.; Gao, F.; Komarneni, S. *J. Am. Chem. Soc.* **2004**, *126*, 54.
- (8) Wang, Y.; Jiang, X.; Xia, Y. *J. Am. Chem. Soc.* **2003**, *125*, 16176.
- (9) Dai, Z. R.; Pan, Z. W.; Wang, Z. L. *Adv. Func. Mater.* **2003**, *13*, 9.
- (10) (a) Law, M.; Kind, H.; Messer, B.; Kim, F.; Yang, P. D. *Angew. Chem., Int. Ed.* **2002**, *41*, 2405. (b) Wang, Y.; Jiang, X.; Xia, Y. *J. Am. Chem. Soc.* **2003**, *125*, 16176.
- (11) He, Y. S.; Campbell, J. C.; Murphy, R. C.; Arendt, M. F.; Swinnea, J. S. *J. Mater. Res.* **1993**, *8*, 3131.
- (12) (a) Harrison, P. G.; Willet, M. J. *Nature* **1988**, *332*, 337. (b) Ferrere, S.; Zaban, A.; Gregg, B. A. *J. Phys. Chem. B* **1997**, *101*, 4490.
- (13) (a) Comini, E.; Faglia, G.; Sberveglieri, G.; Pan, Z. W.; Wang, Z. L. *Appl. Phys. Lett.* **2002**, *81*, 1869. (b) Dai, Z. R.; Gole, J. L.; Stout, J. D.; Wang, Z. L. *J. Phys. Chem. B* **2002**, *106*, 1274.
- (14) (a) Hu, J.; Bando, Y.; Liu, Q.; Golberg, D. *Adv. Func. Mater.* **2003**, *13*, 493. (b) Liu, Z.; Zhang, D.; Han, S.; Li, C.; Tang, T.; Jin, W.; Liu, X.; Lei, B.; Zhou, C. *Adv. Mater.* **2003**, *15*, 1754.
- (15) Zhang, D.-F.; Sun, L.-D.; Yin, J.-L.; Yan, C.-H. *Adv. Mater.* **2003**, *15*, 1022.
- (16) Martin, C. R. *Science* **1994**, *266*, 1961.
- (17) (a) Liu, Y.; Zheng, C.; Wang, W.; Yin, C.; Wang, G. *Adv. Mater.* **2001**, *13*, 1883. (b) Xu, C.; Zhao, X.; Liu, S.; Wang, G. *Solid State Commun.* **2003**, *125*, 301.
- (18) Slater, B.; Catlow, C. R. A.; Gay, D. H.; Williams, D. E.; Dusastre, V. *J. Phys. Chem. B* **1999**, *103*, 10644.
- (19) Oviedo, J.; Gillan, M. J. *Surf. Sci.* **2000**, *463*, 93.
- (20) Leite, E. R.; Giraldo, T. R.; Pontes, F. M.; Longo, E.; Beltrán, A.; Andrés, J. *Appl. Phys. Lett.* **2003**, *83*, 1566.
- (21) (a) Matossi, F. *J. Chem. Phys.* **1951**, *19*, 387. (b) Zuo, J.; Xu, C.; Liu, X.; Wang, C.; Wang, C.; Hu, Y.; Qian, Y. *J. Appl. Phys.* **1994**, *75*, 1835. (c) Abello, L.; Bochu, B.; Gaskov, A.; Koudryavtseva, S.; Lucazeau, G.; Roumyantseva, M. *J. Solid State Chem.* **1998**, *135*, 78.

JA0493244